Investigation of Casson Fluid Flow Past an Enlarging Surface with Thermal Radiation and Heat Source/sink in the presence of Buoyancy Effects

Abhishek Neemawat and Jagdev Singh
Department of Mathematics, JECRC University, Jaipur, India

December 23, 2023

Corresponding Author :jagdevsinghrathore@gmail.com (J.Singh)

Abstract: This study considers in depth the flow of the boundary layer of an incompressible, viscous, and steady Casson fluid through an expanding surface when thermal radiation, heat source, Soret, and Dufour effects are present. Using suitable similarity transformations, the governing non-linear partial differential equations are converted into coupled ordinary differential equations and then estimated using the MATLAB software bvp4c using a shooting process. Variable values of the parameters employed in the current inquiry are offered, together with solutions for the parameters of momentum, temperature, concentration, coefficient of local skin friction, and local Nusselt number. It is observed that the Casson fluid parameter improves fluid velocity and decreases the temperature. Also, it is found that thermal radiation and the presence of a heat source/sink increase the temperature of the fluid. We compared the present investigation with previously published papers and found them harmonious.

Keywords: Casson fluid; Heat source/sink, Thermal radiation; Enlarging sheet; Soret and Dufour effects.

1 Introduction

A few examples of industries where the viscous non-Newtonian fluid in the boundary layer province caused by an expanding flat plate has extensive technical applications include the cooling and drying of paper, aerodynamic extrusion, production of glass fibres, wire drawing, glass blowing, polymer and metal processing industries, and hot rolling.
Nadeem et al. [1] investigated the influences of thermal radiation on a Jeffery fluid's boundary layer along a planar sheet that was expanding exponentially.

They discovered that local skin friction is a declining function of the local suction parameter, and the heat transfer rate is a reducing function of the suction parameter and Eckert number while a rising function of the Prandtl number and radiation parameter. Hiemenz [2] was most likely the first to investigate 2D stagnation flow to transform the NS equations to non-linear ODEs. Crane [3] conducted ground-breaking research on constant boundary layers caused by a linearly expanding sheet. Similarity solutions are also permitted for the flow brought on by stretching sheets, which is significant in extrusion issues. Wang [4] found similar solutions for the axisymmetric situation. The most common fluid model nowadays is the Casson fluid, described as a fluid that thins under shear and has infinite viscosity at zero shear rates. Fredrickson [5] discovered the Casson fluid's continuous flow property in a pipe. Boyd et al. [6] analyzed the oscillatory blood flow while accounting for Casson fluid. They discovered that Casson and Carreau-Yasuda flow display remarkable changes in the steady flow compared to equivalent Newtonian-type flows. Casson fluids are non-Newtonian in nature. The constitutive equation for Casson fluid includes shear stress since it acts like elastic materials like tomato sauce, jelly, soup, honey, and concentrated fruit liquids. Another example of a Casson fluid is human blood. Later on, the MHD flow of a non-Newtonian fluid caused by an exponentially contracting surface was discovered by Nadeem et al. [7]. They found that the issue in the provided situation becomes a Newtonian scenario if the fluid parameter approaches infinity. Casson fluid flow analysis due to a permeable contracting surface with viscous dissipation was explored by Qasim and Nooren [8]. Bhattacharyya et al. [9] created the critical solution of the magnetohydrodynamic porous flow of a Casson fluid along an enlarging sheet. This investigation found that the partial slip strongly affects the velocity. A drop in the mass suction parameter is shown for the Casson fluid flow as the boundary slip parameter is raised. Nandy [10] provided a solution for the MHD Casson fluid flow approaching a stagnation point toward a stretched plate in the presence of a partial slip. To analyse how radiation influenced the fluid mass and heat transfer assessment of a Casson fluid along an unevenly stretched sheet. Swati [11] used the suction and blowing effects. She found that the fluid velocity initially falls when the unsteadiness parameter is raised. Additionally, it is discovered that as the Casson parameter increases, the fluid temperature rises, the fluid velocity field is suppressed, and thermal radiation improves the thermal diffusivity of the fluid, taken into consideration. Peri et al. [12] investigated the dual solutions of Casson fluid flow over a stretching or shrinking sheet. They demonstrated that the Dufour number enhances the velocity and temperature throughout the boundary layer. The concentration boundary layer thickness is enhanced by an increase in the Soret number. The shrinking ratio reduces the velocity of the fluid but enhances the concentration. The skin friction, heat and mass transfer rates increase with the Casson parameter. Many more researchers [13-16] did pioneer work in analytic solutions of ODEs and PDEs and mathematical modeling. Sushila et al. [17] analyzed a hybrid analytical model for thin film in fluid dynamics for non-Newtonian fluids. They found that the homotopy perturbation Elzaki transform method leads over the Elzaki decomposition method

since the non-linear problems are solved without utilizing Adomian polynomials. Moreover, Singh et al.[18] discovered computational analysis of Fractional Lienard's equation with exponential Memory.

The current paper aims to investigate the Casson fluid flow across a stretched sheet. The modified similarity equation's numerical solution is achieved for the stretching sheet. Plots are provided and analyzed in detail for the emerging physical parameters incorporated in the suggested problem.

2 Mathematical construction of the problem

Nakamura and Sawada [19] provided a definition of the rheological equation of Casson fluid flow as given under:

$$\tau_{ij} = \begin{cases} \left(\mu_B + \frac{1}{\sqrt{2\pi}}\tau_y\right) 2e_{ij}, & \pi > \pi_c \\ \left(\mu_B + \frac{1}{\sqrt{2\pi_c}}\tau_y\right) 2e_{ij}, & \pi < \pi_c \end{cases}, \tag{1}$$

where μ_B is used for the Casson fluid's plastic dynamic viscosity, τ_y is taken as the yield stress, π is considered as deformation rate, and it is $\pi = e_{ij}e_{ij}$, where the component of the deformation at $(i,j)^{th}$ position is e_{ij}. τ_c expresses the critical value of π.

Consider 2D steady and incompressible Casson fluid flow near the stagnation point on a permeable enlarging plane surface. The direction of the plane surface is along the X, and the Y axis is taken normal to the surface. The axial velocity components in the above directions are u and v, respectively. The sheet is stretched by applying two equal pressures in the x direction immediately to produce the flow. The plane surface is extended with a linear velocity of the form $u_w(x) = cx$ while preserving the origin fixed, where c is a constant and it is taken as $c > 0$ for an expanding surface, for shrinking sheet $c < 0$ and $c = 0$ for a static surface.

Under the aforementioned assumptions, for this Casson fluid flow, the stable boundary layer equations for incompressible stagnation-point flow are given as follows:

Equation of Continuity:

$$\frac{\partial u}{\partial x} + \frac{\partial u}{\partial y} = 0, \tag{2}$$

Equation of Momentum:

$$u\frac{\partial u}{\partial x} + v\frac{\partial u}{\partial y} = u_e\frac{du_e}{dx} + \nu\left(1 + \frac{1}{\beta}\right)\frac{\partial^2 u}{\partial y^2} + g\beta_T\left(T - T_\infty\right), \tag{3}$$

Equation of Energy:

$$u\frac{\partial T}{\partial x}+v\frac{\partial T}{\partial y}=\alpha_m\frac{\partial^2 T}{\partial y^2}+\frac{D_m K_T}{C_s C_p}\frac{\partial^2 C}{\partial y^2}-\frac{1}{\rho C_p}\frac{\partial q_r}{\partial y}+\frac{Q_0}{\rho C_p}\left(T-T_\infty\right), \tag{4}$$

Equation of Concentration:

$$u\frac{\partial C}{\partial x}+v\frac{\partial C}{\partial y}=D_m\frac{\partial^2 C}{\partial y^2}+\frac{D_m K_T}{T_m}\frac{\partial^2 T}{\partial y^2}-K_0\left(C-C_\infty\right), \tag{5}$$

The following are the borderline circumstances for equations (2) to (5):

$$\left.\begin{array}{l} u=xc,\ \ v=0,\ T-T_\infty=xb,\ C-C_\infty=xd,\ \ when\ y=0,\\ u\to xa,\ \ T\to T_\infty,\ \ C\to C_\infty,\ \ as\ y\to\infty. \end{array}\right\}. \tag{6}$$

where $u_w\left(x\right)=cx$ is the fluid velocity at the wall and c is a constant, $u_e\left(x\right)=ax$ is the ambient fluid velocity where a is a constant, $\beta=\mu_B\sqrt{2\pi_c}/\tau_y$ symbolizes the Casson fluid parameter, β_T is used for the coefficient of thermal expansion, T expresses the fluid temperature, T_w represents the temperature of the sheet, T_∞ is constant, and it is considered as uniform ambient temperature, g is taken as gravitational acceleration, α_m expresses the effective thermal diffusivity, the mean temperature of fluid is T_m, the effective solutal diffusivity is D_m, K_T is used for the ratio of thermal diffusion, C_p is taken as the specific heat at constant pressure, and C_s is the concentration susceptibility.
The stream function ψ is defined as

$$u=\frac{\partial\psi}{\partial y},\qquad v=-\frac{\partial\psi}{\partial x},$$

where $\psi=\sqrt{a\nu}xf\left(\eta\right)$, dimensionless stream function is $f\left(\eta\right)$ and similarity variable is $\eta=y\sqrt{\frac{a}{\nu}}$. Solving this, we get the values of velocity components in both directions are given by

$$\begin{aligned} u&=xaf'\left(\eta\right),\\ v&=-\sqrt{a\nu}f\left(\eta\right). \end{aligned} \tag{7}$$

The Casson fluid temperature and concentration are taken as

$$\theta\left(\eta\right)=\frac{T-T_\infty}{\Delta T}\ \ and\ \ \phi\left(\eta\right)=\frac{C-C_\infty}{\Delta C}, \tag{8}$$

where $\theta\left(\eta\right)$ and $\phi\left(\eta\right)$ are dimensionless temperature and concentration respectively. Equations (2) to (5) become the subsequent two-point boundary value problem when equations (7) and (8) are used:

$$\left(1+\beta^{-1}\right)f'''+ff''-f'^2+\lambda\theta=-1, \tag{9}$$

$$Pr^{-1}\left(1+\frac{4}{3}R\right)\theta''+f\theta'-f'\theta+D_f\phi''+Q\theta=0, \tag{10}$$

$$Sc^{-1}\phi''+f\phi'-f'\phi+Sr\theta''-K\phi=0, \tag{11}$$

The transformed borderline circumstances are:

$$\left.\begin{array}{l} f=0,\ \ f'=\frac{c}{a},\ \ \theta=1,\ \ \phi=1 \quad at\ \ \eta=0, \\ f'\to 1,\ \ \theta\to 0,\ \ \phi\to 0 \quad as \quad \eta\to\infty \end{array}\right\}. \tag{12}$$

where prime ($'$) indicates differentiation with respect to similarity variable η. The non-dimensional parameters used in this article are as follows: $\lambda=\frac{g\beta_T b}{a^2}$ (Buoyancy parameter), $\Pr=\frac{\nu}{\alpha_m}$ (Prandtl number), $Sc=\frac{\nu}{D_m}$ (Schmidt number), $D_f=\frac{D_m K_T(C_w-C_\infty)}{C_s C_p \nu(T_w-T_\infty)}$ (Dufour parameter), $Sr=\frac{D_m K_T(T_w-T_\infty)}{T_m \nu(C_w-C_\infty)}$ (Soret parameter), $R=\frac{4\sigma^* T_\infty^3}{\rho C_p k^* \alpha_m}$ (Radiation parameter), $Q=\frac{Q_0}{a\rho C_p}$ (Heat source/sink parameter) and $K=\frac{K_0}{a}$ (Chemical reaction parameter).

Significant physical entities of a particular flow field, temperature field, and concentration are presented graphically and tabularly in terms of skin friction, local Sherwood number, and Nusselt number, considering engineering and practical value and uses. These are the three measures of attention in the present study.
The surface shearing stress is shown by τ_w and calculated using

$$\tau_w=\left(\mu_B+\frac{\tau_y}{\sqrt{2\pi_c}}\right)\left(\frac{\partial u}{\partial y}\right)_{y=0}=\left(\mu_B+\frac{\tau_y}{\sqrt{2\pi_c}}\right)\sqrt{\frac{a^3}{\nu}}xf''(0), \tag{13}$$

The term for the local skin-friction coefficient is C_f, and its definition is

$$C_f=\frac{\tau_w}{\rho u_e x^2}, \tag{14}$$

Using equation (13) in equation (14), we get

$$Re_x^{1/2}C_f=\left(1+\beta^{-1}\right)f''(0). \tag{15}$$

The formula for the wall's rate of heat transmission is

$$q_w=-k\left(\frac{\partial T}{\partial y}\right)_{y=0}+(q_r)_{y=0}=-k(T_w-T_\infty)\sqrt{\frac{a}{\nu}}\theta'(0)-\frac{16\sigma^* T_\infty^3}{3k^*}(T_w-T_\infty)\sqrt{\frac{a}{\nu}}\theta'(0), \tag{16}$$

The local Nusselt number, represented by the symbol Nu_x, is defined as

$$Nu_x=\frac{xq_w}{k(T_w-T_\infty)}, \tag{17}$$

Using equations (16) and (17), the local Nusselt number can be expressed as follows

$$\frac{Nu_x}{Re_x^{1/2}} = -\left(1+\frac{4}{3}R\right)\theta'(0). \tag{18}$$

q_m stands for the mass flow at the wall and is defined as

$$q_m = -D_s\left(\frac{\partial C}{\partial y}\right)_{y=0} = -\left(C_w - C_\infty\right)D_s\sqrt{\frac{a}{\nu}}\phi'(0), \tag{19}$$

The local Sherwood number is denoted by Sh_x and is defined as

$$Sh_x = \frac{xq_m}{D_s\left(C_w - C_\infty\right)}, \tag{20}$$

Using equations (19) and (20), the Sherwood number can be expressed as follows

$$\frac{Sh_x}{Re_x^{1/2}} = -\phi'(0). \tag{21}$$

Here $Re_x = \frac{xu_e}{\nu}$ is taken as the local Reynolds number.

3 Influence of diverse restrictions on the flow

The given system of coupled ODEs from (9) to (11) with borderline circumstances given in equation (12) was solved using the MATLAB coding package named bvp4c ODEs solver. This portion of the text discusses the effects or influences of several physical non-dimensional parameters on the profiles of energy, momentum, concentration, skin friction, and rate of change of heat transfer. To authorize the outcomes of our numerical method, the values of $\left(1+\beta^{-1}\right)f''(0)$ were compared with values obtained by the researchers Peri [12], Bhattacharyya [20], and Ishak et al. [21] and they are found in very good agreement. Figures in the form of line graphs from 2 to 10 are used to display the distribution of axial velocity, temperature, and concentration. The following is a summary of the findings.

The comparison of the current results to those that have been published is shown in table 1. It is found to an excellent reliability between the present and published results. It also confirms the validity of the method used in the present paper. It can be shown from this table that when stretching parameter values increase, the local skin friction coefficient decreases.

Table 2 contains tabular values of $-\theta'(0)$ for various stretching/shrinking parameter values corresponding to specific fixed values of the other considered parameters. The data show that heat transport reduces as the stretching parameter values increase.

Figure 1 shows that for some fixed values of the stretching parameter, fluid velocity increases as the Casson parameter increases. Also, as the stretching parameter rises, fluid velocity rises in figure 2.

The energy profiles are shown in figures 3 to 7. It is examined that Casson fluid temperature increases as the radiation parameter and heat source parameter increase. Also, temperature decreases for increasing values of the stretching parameter, Prandtl number, and Casson parameter.
Figures 8 and 9 show the concentration distribution of the Casson fluid flow. We noticed that the fluid concentration falls when the stretching parameter and Schmidt number are increased for some fixed values of other parameters.
The effects of temperature and mass distribution on the stretching sheet parameter are depicted in figures 4 and 8. The stretching parameter affects the temperature and mass distributions in the opposite direction. We discovered that the temperature and mass distributions reduce as the stretching parameter increases. This is due to the stretching parameter's direct relationship with the heated fluid's heat transfer coefficient. The amount of convective energy transferred is inversely correlated with the thermal resistance of the warm fluid. As the stretching parameter rises, the warm fluid convection resistance falls, lowering the surface temperature.

4 Conclusion

This paper studies the flow of Casson fluid past an enlarging surface with thermal radiation and heat source/sink in the presence of Buoyancy effects. The Soret and Dufour effects on a Casson fluid are investigated about a stagnation point on a stretching sheet. The momentum, temperature, and concentration equations are written as a system of ordinary differential equations using a suitable similarity transformation and then solved numerically using a code-named MATLAB bvp4c solver. It is found that heat transport reduces as the stretching parameter increases. Also, fluid velocity rises with the Casson and stretching parameters. For the temperature of the fluid, it is seen that it increases with radiation parameter and decreases with increasing Prandtl number and stretching parameter values.
Here are some future scope suggestions for the paper entitled "Investigation of Casson fluid flow past an enlarging surface with thermal radiation and heat source/sink in the presence of buoyancy effects":
1. Examine other non-Newtonian fluid models, apart from Casson fluid, to comprehend how variations in fluid rheology impact the flow properties.
2. Examine the effects of adding nanoparticles to the Casson fluid to produce Casson-based nanofluids. Examine how heat sources, sinks, and thermal radiation affect these nanofluid systems.
3. To capture flow patterns and heat transfer characteristics that are more realistic, expand the current work to three-dimensional simulations. This might offer a more realistic depiction of the actual mechanism.
4. Examine how the system under study affects the environment, considering energy efficiency, sustainability, and possible uses in eco-friendly technologies.

Table 1: Assessment of $\left(1+\frac{1}{\beta}\right) f''(0)$ with Peri [12], Bhattacharyya [20], and Ishak et al. [21] for $\lambda = \Pr = D_f = 0 = Sc = Sr$ and $\beta = 10^8$

c/a	**Present study**	**Peri [12]**	**Bhattacharyya [20]**	**Ishak et al. [21]**
-0.25	1.40224031	1.4022408	1.4022405	1.402241
-0.50	1.49566920	1.4956698	1.4956697	1.495670
-0.75	1.48929749	1.4892982	1.4892981	1.489298
-1.00	1.32881613	1.3288169	1.3288169	1.328817
-1.15	1.08223159	1.0822312	1.0822316	1.082231
-1.20	0.93247562	0.9324734	0.9324728	0.932474
-1.2465	0.58428232	0.5842817	0.5842915	0.584295
0.0	1.23258722	-	-	-
0.2	1.05112962	-	-	-
0.4	0.83407188	-	-	-
0.6	0.58483595	-	-	-
0.8	0.30609469	-	-	-

Table 2: $-\theta'(0)$ for various values of $\beta = 3.5$, $\lambda = 0.01$, $D_f = Sr = Sc = 0.1, \Pr = 0.72, K = Q = R = 0.2$

c/a	$-\theta'(0)$
0.0	1.4034650
0.2	1.19728995
0.4	0.95082859
0.6	0.66793854
0.8	0.35163572
-0.25	1.59653352
-0.5	1.70350740
-0.75	1.69804589
-1.00	1.520163541
-1.15	1.248976011
-1.20	1.08891235
-1.2465	0.81579824

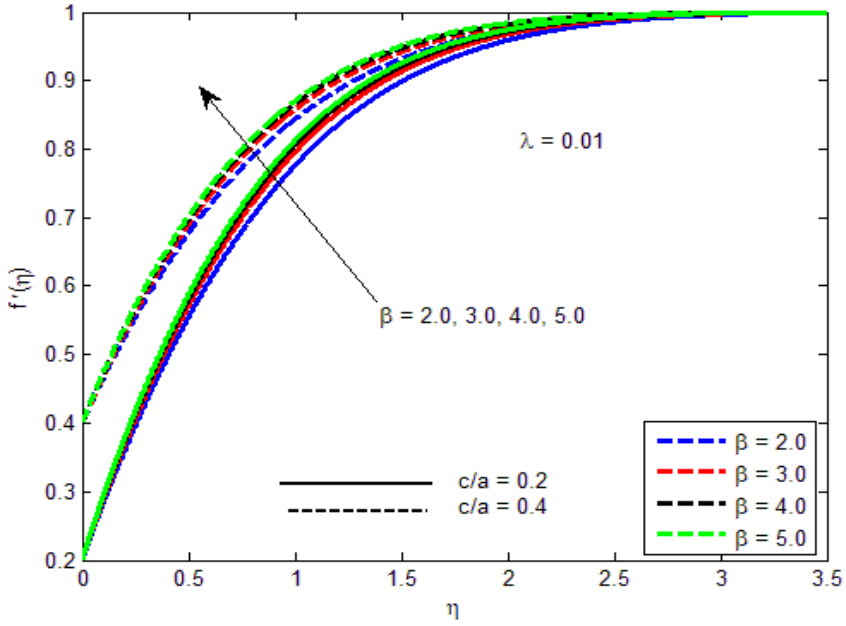

Figure 1: $f'(\eta)$ for unlike facts of β

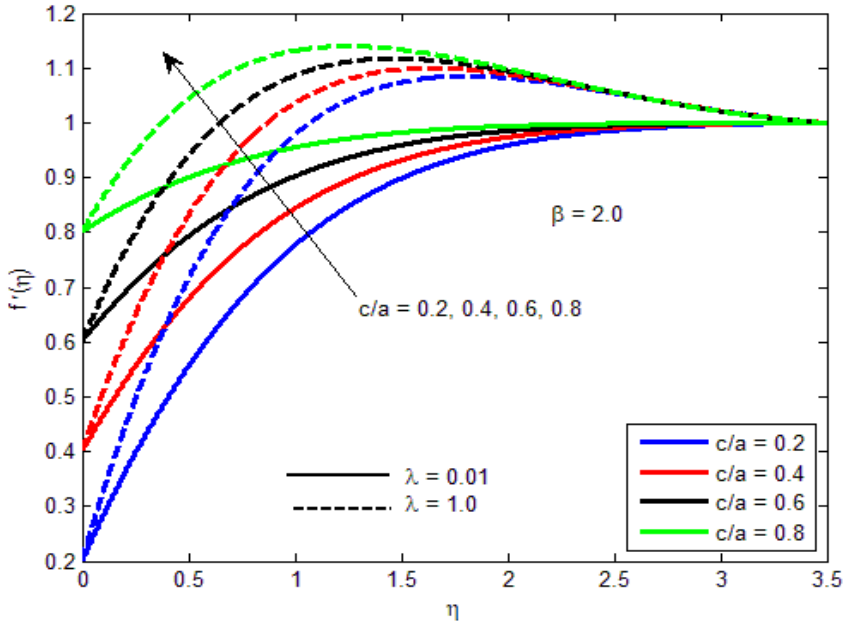

Figure 2: $f'(\eta)$ for unlike facts of c/a

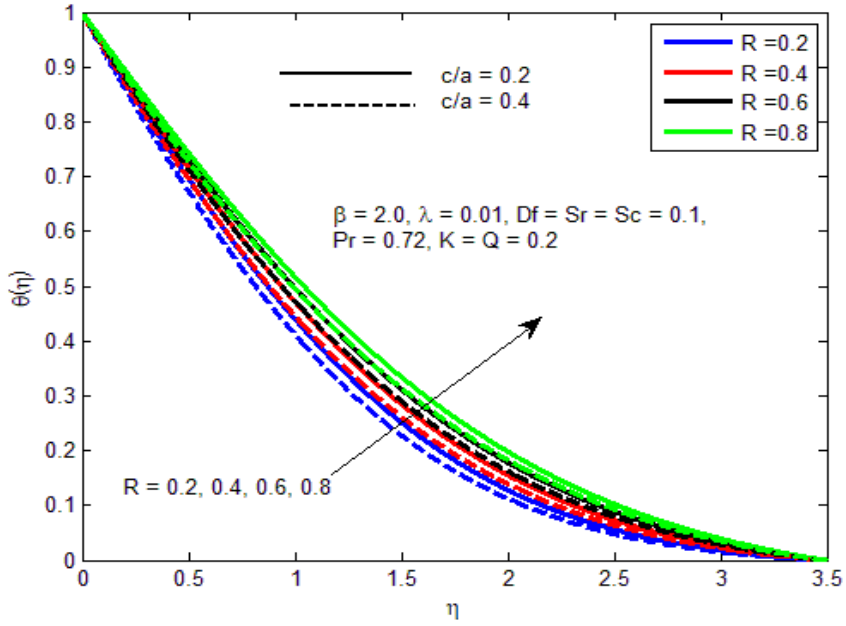

Figure 3: $\theta(\eta)$ for unlike facts of R

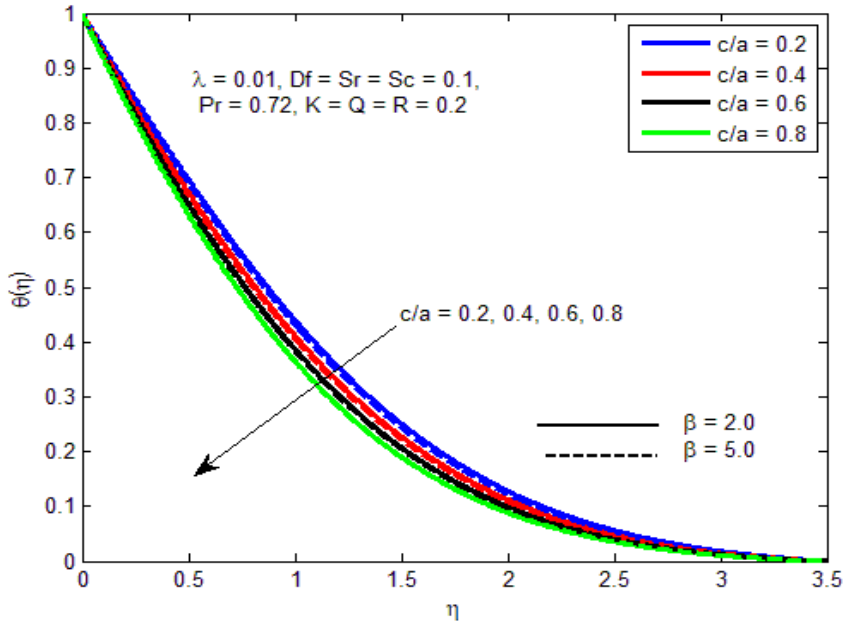

Figure 4: $\theta(\eta)$ for unlike facts of c/a

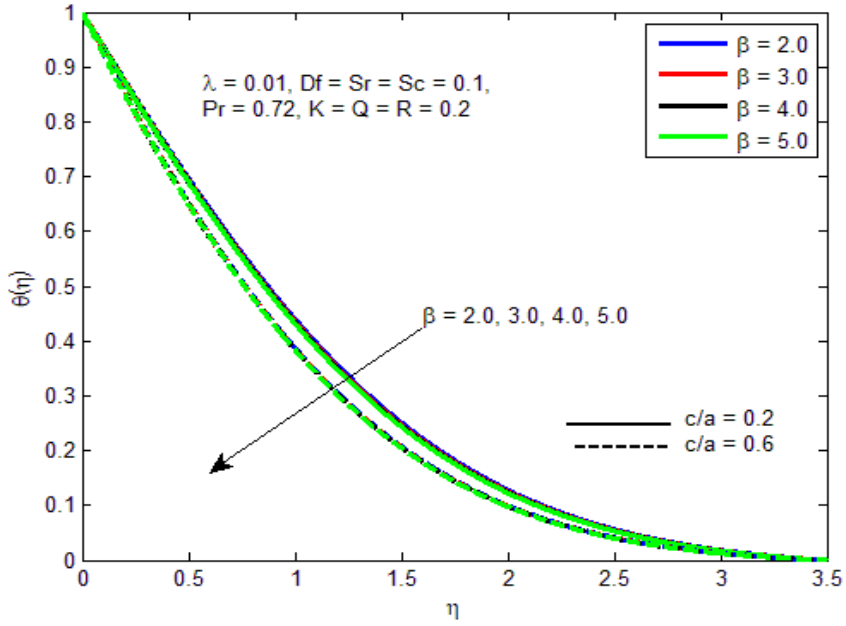

Figure 5: $\theta(\eta)$ for unlike facts of β

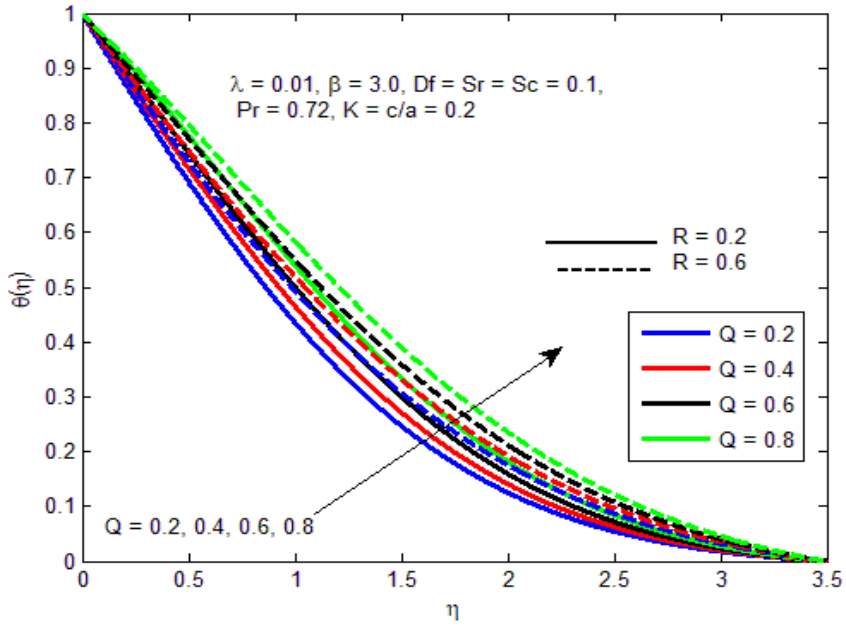

Figure 6: $\theta(\eta)$ for unlike facts of Q

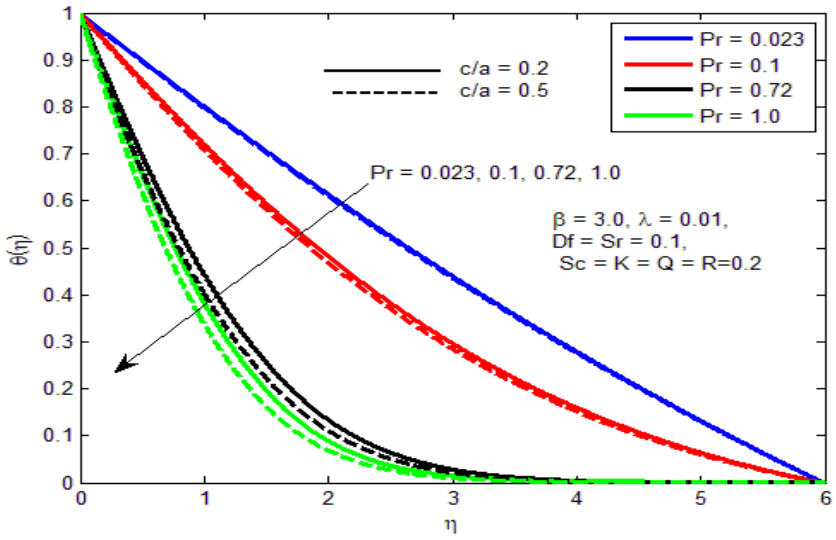

Figure 7: $\theta(\eta)$ for unlike facts of Pr

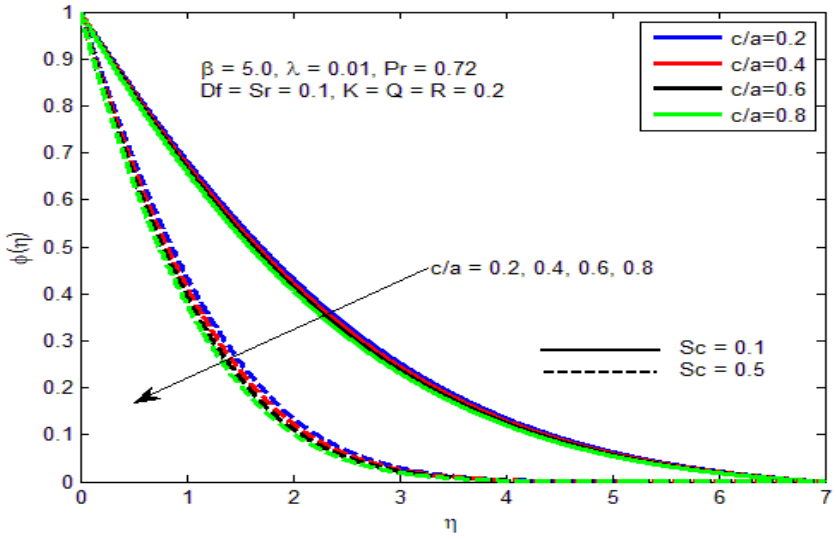

Figure 8: $\phi(\eta)$ for unlike facts of c/a

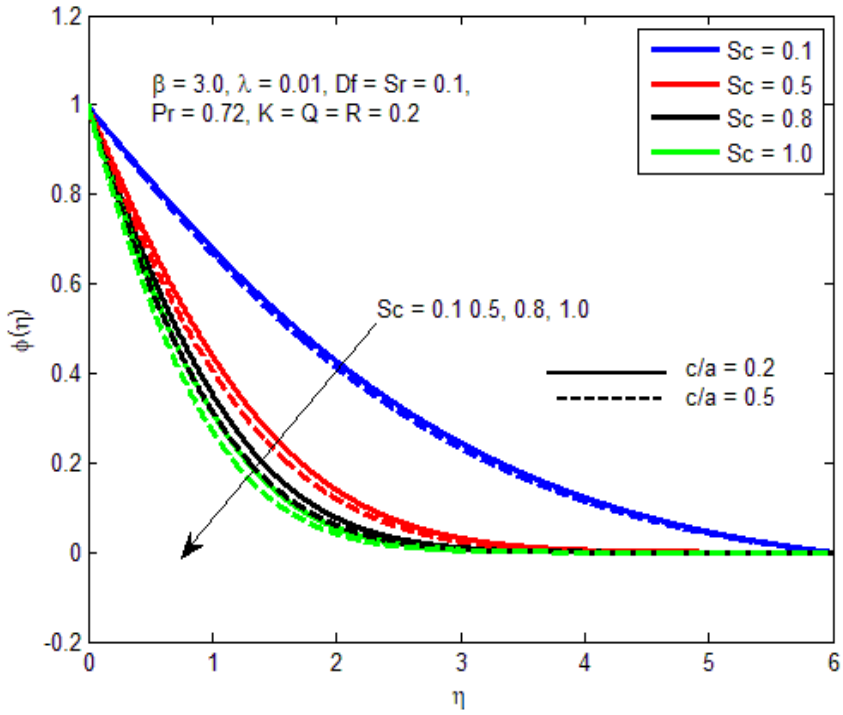

Figure 9: $\phi(\eta)$ for unlike facts of Sc

5 References

[1] Nadeem S., Zaheer S., and Fang T., Effects of thermal radiation on the boundary layer flow of a Jeffery fluid over an exponentially stretching surface, Num. Algor., 2011, 57, 187-205.
[2] Hiemenz K., Die Grenzschicht an einem in den gleichformingen Flussigkeitsstrom eingetauchten graden Kreiszylinder, Dinglers Polytech. J., 1911, 326, 321–324.
[3] Crane L. J., Flow past a stretching plate, Z. Angew. Math. Phys., 1970, 21, 645–647.
[4] Wang C. Y., The three-dimensional flow due to a stretching flat surface, Phys. Fluids, 1984, 27, 1915–1917.
[5] Fredrickson A. G., Principles and applications of Rheology, Prentice-Hall, Englewood Cliffs, N. J., 1964.
[6] Boyd J., Buick J. M., and Green S., Analysis of the Casson and Carreau-Yasuda non-Newtonian blood models in steady and oscillatory flow using the lattice Boltzmann method, Phys. Fluids, 2007, 19, 093103.
[7] Nadeem S., Rizwan U. H., and Lee C., MHD flow of a Casson fluid over an exponentially shrinking sheet, Scientia Iranica B., 2012, 19, 1550-1553.
[8] Qasim M., and Noreen S., Heat transfer in the boundary layer flow of a

Casson fluid over a permeable shrinking sheet with viscous dissipation, Eur. Phys. J. Plus, 2014, 7, 129.
[9] Bhattacharya K., Vajravelu K., and Hayat T., Slip effect on parametric space and the solution for the boundary layer flow of Casson fluid over a non-porous stretching/shrinking sheet, Int. J. Fluid Mech. Research, 2013, 40, 482-493.
[10] Nandy S. K., Analytical solution of MHD stagnation-point flow and heat transfer of Casson fluid over a stretching sheet with partial slip, ISRN Thermodynamics, 2013, Article ID 108264, 9 pages.
[11] Mukhopadhyay S., Effect of thermal radiation on Casson fluid flow and heat transfer over unsteady stretching surface subject to suction/blowing, Chin. Phys. B., 2013, 22, 1-7.
[12] Peri K., Shaw S., and Sibanda P., Dual solutions of Casson fluid flow over a stretching or shrinking sheet, Sadhana, 2014, 39, Part 6, 1573–1583.
[13] Kumar D., Dubey V. P., Dubey S., Singh J. and Alshehri A. M., Computational analysis of local fractional partial differential equations in Realm of fractal calculus, Chaos, Solitons and Fractals 167, 2023, 113009.
[14] Dubey V. P., Singh J., Alshehri A. M., Dubey S. and Kumar D., Analysis and fractal dynamics of some local fractional partial differential equations occurring in physical sciences, J. Comput. Nonlinear Dynam. 18(3), 2023, 1-23.
[15] Dubey V. P., Singh J., Alshehri A. M., Dubey S. and Kumar D., Analysis of Cauchy problems and diffusion equations associated with the Hilfer-Prabhakar fractional derivative via Kharrat-Toma transform, Fractal and Fractional, 2023, 7(5)413, 1-16, https://doi.org/10.3390/fractalfract7050413.
[16] Dubey V. P., Singh J., Alshehri A. M., Dubey S., and Kumar D., Forecasting the behavior of fractional order Bloch equations appearing in NMR flow via a hybrid computational technique, Chaos Solitons Fract., 2022, 164, 112691.
[17] Sushila, Singh J., Kumar D. and Baleanu D., A hybrid analytical algorithm for thin film problem occurring in non-Newtonian fluid mechanics, Ain Shams Engineering Journal, 2021, 12 (2), 2297-2302.
[18] Singh J., Alshehri A. M., Sushila and Kumar D., Computational analysis of fractional Lienard's equation with exponential memory, Journal of Computational and Nonlinear Dynamics, ASME (The American Society of Mechanical Engineers), 2023, 18(4), 041004, https://doi.org/10.1115/1.4056858.
[19] Nakamura M. and Sawada T., Numerical study on the flow of a non-Newtonian fluid through an axisymmetric stenosis, J. Biomech. Eng., 1988, 110, 137–143.
[20] Bhattacharyya K., Dual solutions in boundary layer stagnation-point flow and mass transfer with chemical reaction past a stretching/shrinking sheet, Int. Commun. Heat Mass Transf., 2011, 38, 917–922.
[21] Ishak A., Lok Y. Y. and Pop I., Stagnation-point flow over a shrinking sheet in a micropolar fluid, Chem. Eng. Comm., 2010, 197, 1417–1427.